

# Dynamics of transpiration and evaporation following a moisture pulse in semiarid grassland: A chamber-based isotope method for partitioning flux components

Enrico A. Yepez<sup>a,\*</sup>, Travis E. Huxman<sup>b</sup>, Danielle D. Ignace<sup>b</sup>,  
Nathan B. English<sup>c</sup>, Jake F. Weltzin<sup>d</sup>, Alejandro E. Castellanos<sup>e</sup>,  
David G. Williams<sup>f</sup>

<sup>a</sup>School of Natural Resources, University of Arizona, Tucson, AZ 85721, USA

<sup>b</sup>Ecology and Evolutionary Biology, University of Arizona, Tucson, AZ 85721, USA

<sup>c</sup>Department of Geosciences, University of Arizona, Tucson, AZ 85721, USA

<sup>d</sup>Ecology and Evolutionary Biology, University of Tennessee, Knoxville, TE 37919, USA

<sup>e</sup>DICTUS, Universidad de Sonora, Hermosillo Sonora, 83000, Mexico

<sup>f</sup>Departments of Renewable Resources and Botany, University of Wyoming, Laramie, WY 82071, USA

Received 16 May 2005; accepted 14 September 2005

## Abstract

We describe a novel method for partitioning evapotranspiration (ET) from isotopic measurements of water vapor within large (4.86 m<sup>3</sup>) plot-scale gas exchange chambers. Using this approach, the short-term (15-day) dynamics of transpiration (*T*) and evaporation (*E*) in experimental replicated stands of the invasive grass *Eragrostis lehmanniana* and the native *Heteropogon contortus* were assessed following a 39-mm irrigation event in semiarid grassland in southeastern Arizona, USA. Water vapor samples (20–40 μL each) were collected sequentially during a 6-min transient increase of vapor concentration inside the chambers and used to produce Keeling plots (isotope mixing relationships) for identification of the isotopic composition of ET and partitioning of component fluxes. The method worked well in plots free of grass cover and in the sparsely covered plots of *E. lehmanniana*. Keeling plot estimates of the isotopic composition of soil evaporation ( $\delta_E$ ) in bare plots closely matched modeled values, lending strong support for the validity of the chamber approach. *T/ET* increased in stands of *E. lehmanniana* from  $0.35 \pm 0.07$  on day 1 to  $0.43 \pm 0.08$  on day 3 after the irrigation pulse, but decreased to  $0.22 \pm 0.05$  by day 7 as the soil surface dried. Estimates of stand transpiration from the Keeling plot chamber method were positively correlated (Pearson's  $r = 0.76$ ,  $p = 0.0004$ ,  $n = 17$ ) with independent estimates based on leaf-to-canopy scaling of stomatal conductance. We were unable to calculate *T/ET* on days 1 and 3 in plots of *H. contortus* because Keeling plot intercepts did not fall within the range of soil and canopy end-member isotope values. This likely occurred due to unaccounted effects of a wet litter layer on the estimation of  $\delta_E$ . Our approach is useful for partitioning ET over a dynamic wetting event in semi-arid grassland at a scale relevant for experimental ecosystem studies, but requires further validation under a wide range of vegetation structures and environmental conditions.

© 2005 Elsevier B.V. All rights reserved.

**Keywords:** Keeling plots; Water vapor; Precipitation pulses; Water isotopes; *Eragrostis lehmanniana*; *Heteropogon contortus*; Santa Rita Experimental Range

\* Corresponding author. Present address: Department of Renewable Resources, University of Wyoming, Laramie, WY 82071-3354, USA. Tel.: +1 307 766 2603; fax: +1 307 766 6403.

E-mail address: [yepezglz@ag.arizona.edu](mailto:yepezglz@ag.arizona.edu) (E.A. Yepez).

## 1. Introduction

Arid and semiarid ecosystems are characterized by infrequent precipitation events and highly variable soil moisture. Episodic increases in resource availability in these ecosystems trigger active, but short-lived periods of soil nutrient cycling and biosphere-atmosphere exchange of materials and energy (Austin et al., 2004; Huxman et al., 2004a). Water from growing-season precipitation is rapidly lost from the rooting zone by transpiration or soil evaporation depending, in part, on the size of the precipitation event (Loik et al., 2004) and structural and physiological characteristics of the vegetation (Huxman et al., 2004a). From an ecophysiological perspective, characterizing the rapid changes in plant transpiration and soil evaporation during these dynamic wetting and drying cycles will help to resolve the linkages between precipitation and ecosystem production (Huxman et al., 2005), and the role of vegetation in controlling water balance (Scanlon et al., 2005).

The ratio of transpiration ( $T$ ) to evapotranspiration (ET) is a synthetic parameter that integrates ecophysiological and microenvironmental controls on total ecosystem water exchange (Reynolds et al., 2000), and provides insight into mechanisms linking the carbon and water cycle. This parameter is often approximated with modeling or with empirical measurements made at unmatched spatial and temporal scales (Reynolds et al., 2000; Wilson et al., 2001). For instance, micrometeorological techniques integrate ET fluxes over large areas, but often lack information on ET components (Moncrieff et al., 2000). In contrast, up-scaling gas exchange measurements from plants and soil surfaces is challenging due to the heterogeneous nature of natural ecosystems (Percy et al., 1989; Kostner, 2001). Both approaches have limitations in experimental ecosystem studies where plot size is often small and the demand for measurement replication is high.

The use of stable isotope techniques to scale and partition  $\text{CO}_2$  and water fluxes is now common in terrestrial ecosystem studies (Yakir and Sternberg, 2000). Stable isotope measurements offer valuable information on the sources of and processes influencing ET (Wang and Yakir, 2000). When combined with flux measurements (Williams et al., 2004) and/or process-based ecosystem models (Riley et al., 2003) isotope measurements provide unique information about the biophysical controls on ecosystem gas exchange.

Dynamic changes in  $T/ET$  can be estimated from the isotopic composition of water vapor in the ecosystem boundary layer and that of the sources of ecosystem

water flux. Water added to the ecosystem air from ET carry the unique isotopic signal(s) from plants and soil (Wang and Yakir, 2000). By knowing the isotopic signal of plant transpiration and soil evaporation ( $E$ ), the relative contributions of  $E$  and  $T$  to total ET can be determined. Isotopic mass balance is used to estimate these fractions (Yakir and Sternberg, 2000):

$$\frac{T}{ET} = \frac{\delta_{ET} - \delta_E}{\delta_T - \delta_E} \quad (1)$$

where  $\delta_{ET}$  is the isotopic composition of evapotranspiration determined with a Keeling plot of water vapor (Keeling, 1961; Wang and Yakir, 2000);  $\delta_T$ , the isotopic composition of transpiration (Flanagan et al., 1991; Farquhar and Cernusak, 2005) and  $\delta_E$  is the heavily fractionated isotopic composition of the vapor from soil evaporation (Craig and Gordon, 1965; Gat, 1996). Keeling plots of water vapor have been used successfully to describe ecosystem-level water relations in tropical and temperate forest (Moreira et al., 1997; Harwood et al., 1999), herbaceous and woody crops (Wang and Yakir, 2000; Williams et al., 2004), a semiarid woodland (Yopez et al., 2003) and a sub-humid temperate grassland (Helliker et al., 2002).

In this paper, we present a method for determining instantaneous  $T/ET$  values from Keeling plots of water vapor generated within a static, plot-scale gas exchange chamber. We demonstrate the applicability of the method by describing the short-term patterns of ET and  $T/ET$  in experimental grassland plots following a large irrigation pulse.

## 2. Materials and methods

### 2.1. Experimental grassland plots and irrigation

Short-term patterns of ET and  $T/ET$  were measured in experimental plots (1.8 m × 1.5 m) of the African invasive grass *Eragrostis lehmanniana* Ness. and the native grass *Heteropogon contortus* (L.) Beauv. growing under rain-out shelters at the Santa Rita Experimental Range (SRER) in southeastern Arizona, USA (English et al., 2005; 31°78'N, 100°88'W). Replicated grass-covered plots of each species were arranged in three rain-out shelters. Measurements were made also on two bare plots where the only possible source of ET was soil evaporation. Soil at this study site is a coarse, loamy-sand with 6% clay. The experimental plots used in this study had received experimental precipitation regimes for 2 years that closely matched the long-term precipitation average (English et al., 2005). We hand-

irrigated each plot with 39 mm of water at the start of the growing season (June 12) in 2003 to simulate a large precipitation event. As part of a larger effort to understand dynamics of plant water uptake in grasses and tree seedlings following water manipulations in the experimental plots (e.g. Fravolini et al., 2005), irrigation water used in our study was highly enriched with  $^2\text{H}$ , which produced a  $\delta^2\text{H}$  value of +143‰. Labeling is not necessarily required for ET partitioning using the Keeling plot approach.

## 2.2. Evapotranspiration measurements

Instantaneous ET rates were measured twice daily in each plot on days –1, 1, 3, 7 and 15 with respect to the watering treatment (hereafter designated D–1, D1, D3, D7 and D15). Measurements were made in the morning between 8:30 and 11:30 h (local time) and in the afternoon between 14:00 and 16:30 h. ET was measured using a large (4.86 m<sup>3</sup>), plot-sized gas exchange chamber similar to the one used in Huxman et al. (2004b). Chamber materials were the same as those described in Arnone and Obrist (2003). The chamber was fitted tightly to the ground surface onto 5-cm high permanent boarders delimiting plot boundaries and was sealed by pressing side sleeves to the ground with a heavy steel chain. ET rates were calculated from the slope of incremental increases in water vapor concentration inside the chamber through time (mmol H<sub>2</sub>O s<sup>-1</sup>). Vapor concentration was measured with an infrared gas analyzer (IRGA; LI-7000, Li-Cor Inc., Lincoln, NE, USA) configured in a closed loop with the chamber. Three 625-cm<sup>2</sup> 12-V DC fans fitted to a tripod mixed the air inside the chamber. The air was drawn through low absorption tubing (3 mm i.d.; Bev-a-Line IV, Thermoplastic Inc., Stirling, NJ, USA) with a small diaphragm pump (Gast Inc., Benton Harbor, MI, USA) for sampling at a flow rate of 3 L min<sup>-1</sup> (measured with a direct reading flow meter; Gilmont Instruments, Barrington, IL, USA). Air temperature inside the chamber was measured at 1-s intervals with a shielded, fine-wire copper-constantan thermocouple. Each ET measurement lasted 6 min, which resulted in an increase of water vapor concentration of approximately 10–15 mmol mol<sup>-1</sup> and an increase of air temperature of typically 1 °C.

## 2.3. Evapotranspiration flux partitioning

### 2.3.1. Vapor collection for Keeling plot analysis

We calculated  $T/ET$  during measurements of ecosystem gas exchange based on isotopic mass balance

(Eq. (1)). Keeling plots of water vapor were used to determine  $\delta_{\text{ET}}$  (Wang and Yakir, 2000). Keeling plots were obtained by regressing the isotopic composition ( $\delta^2\text{H}$ ) of five vapor samples withdrawn from the chamber at different time intervals against the inverse of the vapor concentrations inside the chamber during the gas exchange measurements. For this relationship, the y-intercept of the best-fit line indicated  $\delta_{\text{ET}}$ . Errors from the measurements of the isotopic composition and the vapor concentration were calculated for the intercept using a geometric mean regression (Sokal and Rohlf, 1995). The standard error of the intercept was calculated with estimates from the original regression (model I; Sokal and Rohlf, 1995). We further used estimates of  $T/ET$  from the chamber method to calculate instantaneous rates of stand transpiration from each stand by multiplying  $T/ET$  times the net evapotranspiration rate (e.g.  $T = T/ET \times ET$ ).

Water vapor collection for isotope analysis was made with a five-port cryogenic vapor trapping system (Fig. 1). The trapping system consisted of a set of 10-paired electronic solenoid valves (Clippard Inc. Cincinnati, OH, USA), a datalogger (CR23x, Campbell scientific, Logan UT, USA), an array of five solid-state relays (DC60S3, Crydom Corp., San Diego, CA, USA) and a cold ethanol bath holding five 25-cm long glass vapor traps (modified from Helliker et al., 2002). The ethanol was kept at –80 °C with frequent additions of liquid nitrogen. Vapor collection started 10 s after the chamber was placed and sealed to the ground for gas exchange measurements (see above). During the gas exchange measurements, the datalogger-controlled relays opened and closed paired valves every 70 s to route air flow sequentially through each of the five glass traps. Opened valves allowed constant flow (3 L min<sup>-1</sup>) to one trap at a time. Traps were completely isolated from the loop and from background air when valves were closed. Individual traps collected between 20 and 40  $\mu\text{L}$  of water, depending on the ET rates and the position in the collection sequence during gas exchange measurements. After the complete 6-min interval, traps were removed from the bath and immediately sealed with a rubber stopper and Parafilm. Samples were then wrapped in aluminum foil and stored at 2 °C in a dry insulated cooler for transport to the lab.

### 2.3.2. Isotopic composition of transpiration

The isotopic composition of transpiration ( $\delta_T$ ; Eq. (1)) was calculated from modeled values of leaf water enrichment under non-steady state conditions (Farquhar and Cernusak, 2005):

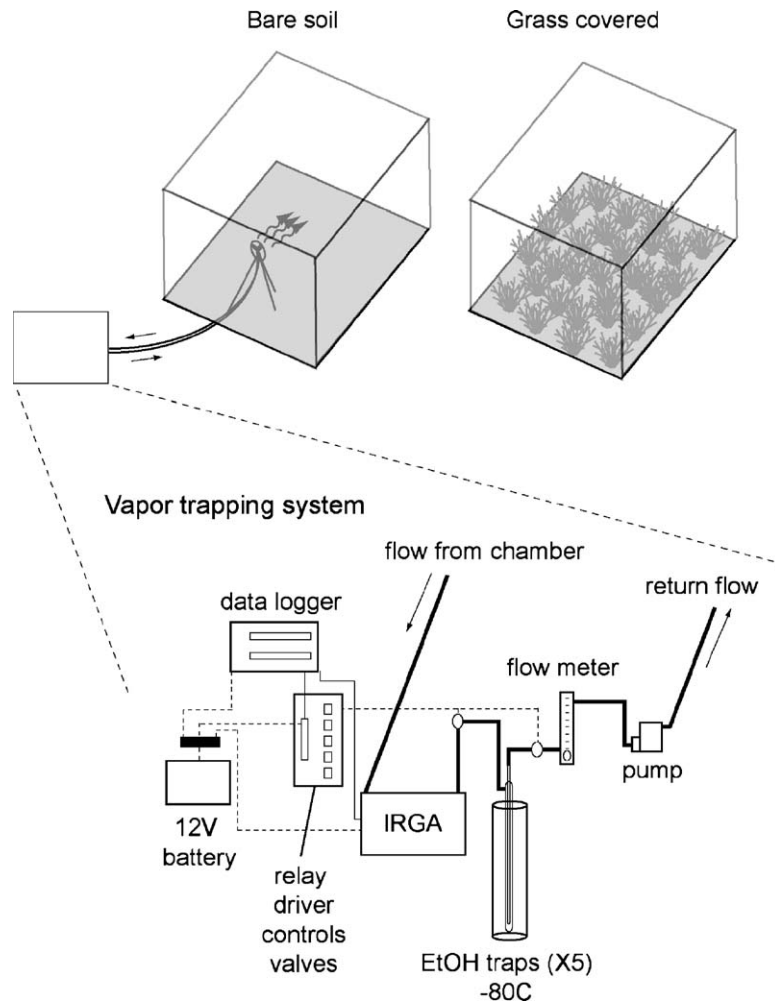


Fig. 1. Diagram of gas exchange and vapor trapping system used to measure ET rates and to collect water vapor for stable isotope analysis. For clarity, only one of the five glass vapor traps is shown.

$$\Delta_{en} = \Delta_{es} - \left[ \frac{d(W\Delta_{en})/dt}{gw_i} \right] \quad (2)$$

where  $\Delta_{en}$  is the isotopic enrichment of leaf water under non-steady state conditions;  $\Delta_{es}$ , the isotopic enrichment of leaf water at steady state (Craig and Gordon, 1965);  $W$ , the relative leaf water concentration ( $\text{mol m}^{-2}$ );  $g$ , stomatal conductance ( $\text{mol m}^{-2} \text{s}^{-1}$ );  $t$ , time (s) and  $w_i$ , the mole fraction of leaf water (e.g. vapor saturation at leaf temperature/atmospheric pressure). The leaf evaporative water enrichment at isotopic steady state was calculated as (Cernusak et al., 2002):

$$\Delta_{es} = \varepsilon^* + \varepsilon_k + (\Delta_a - \varepsilon_k) \frac{e_a}{e_i} \quad (3)$$

where  $\varepsilon^*$  is the temperature-dependent equilibrium fractionation factor in permil;  $\varepsilon_k$ , the kinetic fractionation factor for  $\delta^2\text{H}$  (16.4‰; Cappa et al., 2003);  $\Delta_a$ , the isotopic discrimination between ambient vapor surrounding the leaf and source (stem) water ( $\Delta_a = R_a/R_s - 1$ , where  $R_a$  and  $R_s$  are molar ratios of heavy to light isotopes of vapor and stem water, respectively);  $e_a$ , the ambient vapor pressure and  $e_i$  is the vapor pressure at the intercellular leaf spaces (e.g. saturation vapor pressure at leaf temperature).

The isotopic composition of transpiration relative to the source water was then calculated as (Farquhar and Cernusak, 2005):

$$\Delta T = \frac{\Delta_{en} - \Delta_{es}}{\alpha_r \alpha^* (1 - h)} \quad (4)$$

where  $\Delta T$  denotes the isotopic composition of transpired vapor expressed as deviation beyond the source (stem) water;  $\alpha_k$ , the kinetic fractionation factor for hydrogen (1.016; Cappa et al., 2003);  $\alpha^*$ , the equilibrium fractionation factor (Majoube, 1971); and  $h$ , the relative humidity normalized to the leaf temperature.

Eqs. (2)–(4) were parameterized with  $g$  data for the grasses (see Section 2.5) and microclimate measurements to develop predictions of  $\Delta T$  for each whole-plot gas exchange measurement period. Eq. (2) was solved iteratively for three periods during the day using the Solver function from Microsoft Excel. The model was initialized for each vegetation plot at 7:00 h, 2 h before the first gas exchange measurement.  $\Delta n$  at this time was assumed to be 40‰ (Cernusak et al., 2002). The average relative water content of three leaves collected at predawn was used for the initial value of  $W$ . We used average values of  $W$  measured at 9:00, 12:00 and 16:00 h on three leaves per species for the remainder of the iterations. The daily average  $W$  for *E. lehmanniana* was  $7.9 \pm 1 \text{ mol m}^{-2}$  and for *H. contortus* was  $8.7 \pm 1.6 \text{ mol m}^{-2}$  with the standard deviation indicating the difference between  $W$  values at predawn and those at 16:00 h. In all simulations, we assumed fixed time intervals for all plots. Such intervals roughly corresponded to the average time between 7:00, 9:00, 12:00 and 16:00 h.

We used the isotopic composition of the first vapor sample collected from the static chamber for  $R_a$  in Eq. (3). We used the values corresponding to each plot for morning and afternoon while the average of these two periods was used for the midday iteration. We collected small (~3-cm long) portions of shoot bases near the ground surface from three different grasses growing inside each experimental plot at midday of each measurement day for estimates of  $R_s$ . Grass samples were combined into a single sample within each plot and then placed into screw-cap glass vials and sealed with Parafilm.

### 2.3.3. Isotopic composition of the soil evaporation flux

We collected soil samples from six depths (0–2, 2–4, 4–6, 6–10, 10–20 and 20–30 cm) within each plot on each sampling day to determine the water content and the isotopic composition of water for calculations of  $\delta_E$  (Eq. (1)). Soil samples in the field were handled similarly to the stems. The soil moisture profiles were used to identify soil layers where liquid water was available for evaporation, defined here as the transition zone between liquid and vapor diffusion (van de Griend and Owe, 1994; Yamanaka and Yonetani, 1999; Whythers et al., 1999).

This region occurred near the soil surface shortly after irrigation, but as the topsoil dried the evaporation front deepened in the soil profile. Liquid diffusion in the soil is limited by a critical matric potential ( $\Psi_{me}$ ); below this critical value (more negative matric potential) water transport takes place only as vapor. In coarse sand;  $\Psi_{me}$  occurs at about  $-7 \text{ MPa}$  (at  $0.02 \text{ m}^3 \text{ m}^{-3}$  volumetric water content) while liquid diffusion is at maximum around  $-0.2 \text{ MPa}$  ( $0.09 \text{ m}^3 \text{ m}^{-3}$ ) (Konukcu et al., 2004). We assumed that the upper boundary of a 10 cm thick evaporation front occurred within this transition zone in the sandy soils in our experimental plots and used a soil water potential of  $-3.6 \text{ MPa}$  ( $0.027 \text{ m}^3 \text{ m}^{-3}$  or 10% below the water content where  $\Psi_{me}$  occurs in coarse sand) as a threshold value to indicate the top of the evaporation front. We used the average isotopic values of soil water from these layers in each plot for the calculations of  $\delta_E$  (below). We used the average values from 0 to 10 cm on D1 and D3 and the value from the 10–20 cm layer on D7 (Fig. 2). The soil profile was too dry in all plots on D15 and none of the layers from 0 to 30 cm met our criteria for estimating  $\delta_E$ . Therefore, we did not compute  $\delta_E$  on D15. We further compared the isotopic composition of grass source water (xylem water in basal culms) with the isotope values of water from our assumed evaporation front to determine if grass source water values would serve as a suitable proxy for the isotopic composition of water at the evaporation front (Wang and Yakir, 2000).

$\delta_E$  ( $\delta^2\text{H}$ ) was calculated based on Craig and Gordon (1965) formulation that accounts for equilibrium and kinetic fractionation during phase change and diffusion of water vapor to the mixed boundary layer near the soil surface. The expression for the overall fractionation in delta notation (‰) is provided in Wang and Yakir (2000):

$$\delta_E = \frac{\alpha^* \delta_L - h \delta_a - \varepsilon^* - (1-h)\varepsilon_k}{(1-h) + (1-h)(\varepsilon_k/1000)} \quad (5)$$

where  $\delta_E$  is the isotopic composition water evaporated from the soil;  $\delta_L$ , the isotopic composition of liquid water at the evaporating front; and  $\delta_a$ , the isotopic composition of the background atmospheric water vapor.  $\alpha^*$  is the temperature-dependent equilibrium fractionation factor for  $^2\text{H}$  [ $\alpha^* = (24.844(10^6/T_{\text{soil}}^2) - 76.248(10^3/T_{\text{soil}}) + 52.612)/1000 + 1$ ] with  $T_{\text{soil}}$  in degrees Kelvin (Majoube, 1971).  $\varepsilon^* = (1 - \alpha^*) \times 10^3$ .  $\varepsilon_k$  is the kinetic fractionation factor for hydrogen (16.4‰ for non-turbulent conditions and 10.9‰ for turbulent transport; Cappa et al., 2003); and  $h$ , the relative humidity normalized to the temperature

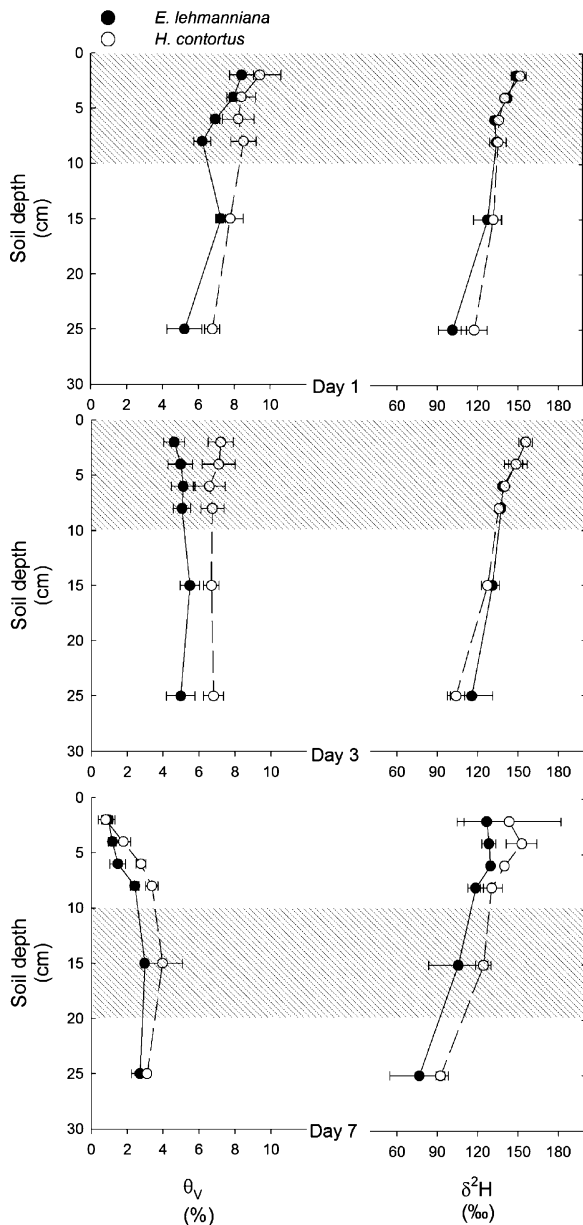


Fig. 2. Surface soil volumetric water content ( $\theta_v$ ) and corresponding  $\delta^2\text{H}$  profiles in experimental stands of *Eragrostis lehmanniana* (dark symbols) and *Heteropogon contortus* (open symbols) on three different days following an experimental irrigation. Bars are the standard errors of the mean ( $n=3$ ). Shaded regions indicate the assumed evaporation front for calculations of  $\delta_E$ .

of the soil surface.  $\delta_E$  estimates were made using the average soil temperature recorded at 5 cm depth in three randomly chosen locations inside each stand prior to the gas exchange measurement to calculate  $\alpha^*$  and normalize  $h$ , the isotopic composition of liquid soil water at the evaporation front and the initial isotopic composition of

vapor inside the chamber (e.g. the value of the first vapor sample withdrawn from the chamber). Turbulent conditions for evaporation were assumed to occur only when the surface soil layers were visually wet; 10.9‰ was used for  $\epsilon_k$  on D1 in stands of *E. lehmanniana*.

#### 2.4. Isotope analysis

Water extraction of soils and stems for isotope analysis was carried out by cryogenic vacuum distillation (Ehleringer et al., 2000). Similarly, water vapor from gas exchange was quantitatively distilled to flame-sealed Pyrex tubes for storage within a few days after collection. Following the extraction, the volumetric water content ( $\theta_v$ ) of the soil samples was determined based on the change in weight of each sample and the bulk density of the soil.  $\delta^2\text{H}$  values of vapor, soils and stem water were measured with a dual-inlet isotope ratio mass spectrometer (Optima, Micromass Ltd., Manchester, UK) at the University of Wyoming Stable Isotope Facility following an offline reduction with zinc (Coleman et al., 1982). Reported values are in per mil (‰) relative to V-SMOW. Precision for our method based on repeated analysis of working standards was 1.2‰.

#### 2.5. Grass water relations and leaf-to-canopy scaling

Predawn shoot water potentials were determined on one individual grass plant per plot on (D–1, D1 and D3 with a Scholander-type pressure chamber (PMS Instrument Co., Corvallis, OR, USA). Stomatal conductance ( $g$ ) was measured at morning, midday and afternoon in grasses from all plots during the same days on which stand-level gas exchange was determined. Measurements were made on one fully expanded sun-lit leaf per plot with a LI-6400 photosynthesis system (Li-Cor Inc., Lincoln, NE, USA), where temperature, photosynthetically active radiation and humidity in the chamber were set to match ambient conditions. Canopy temperatures were determined with an infrared thermometer at the time of stomatal conductance measurements.

We estimated canopy light interception as an indirect index of canopy cover (e.g. live and dead standing biomass) on each plot prior to the irrigation with a 1-m line quantum sensor (Li-191, Li-Cor Inc., Lincoln, NE, USA). After one above-canopy (1.5 m) reading, the sensor was inserted above leaf litter but below any standing blades of grass. Three light measurements were taken perpendicular to the long axis of each plot at

approximately 1/4, 1/2, and 3/4 along the axis. The mean difference between these three readings and the above canopy reading was computed as the light canopy interception. Green leaf area (LAI;  $\text{m}^2 \text{m}^{-2}$ ) from each plot was determined as in Huxman et al. (2004b) by multiplying the mean individual tiller's leaf area by the mean number of live tillers per individual and plant density in a given stand. We scaled leaf-level transpiration to canopy transpiration rates based on the measurements of LAI,  $g$ , canopy temperature and the difference in vapor pressure between the air and canopy (Percy et al., 1989). Estimates of canopy transpiration from this method were compared with those from the stable isotope chamber method at corresponding times (Section 2.3).

### 3. Results

#### 3.1. Soil water budget and evapotranspiration

The soil volumetric water content ( $\theta_v$ ) from 0 to 30 cm depth increased in all experimental plots following the 39-mm irrigation, but decreased to original levels within 15 days.  $\theta_v$  was higher in stands of *H. contortus* than in stands of *E. lehmanniana* during the first week after the wetting event (Fig. 2). The isotopic composition of water within the soil profile during the first 3 days following the wetting event was similar between plots covered with the two grass species. Values from the top 10 cm were very similar to that of the irrigation label (+143‰) suggesting that the irrigation water was the dominant source of water in the surface layers but mixed at a slower rate with less enriched water at lower depths (Fig. 2). Soil water in stands of *H. contortus* by D7 had a more positive  $\delta^2\text{H}$  value compared to that in stands of *E. lehmanniana* (Fig. 2). The greater isotopic enrichment of soil water in *H. contortus* stands compared to *E. lehmanniana* stands on D7 indicates that proportionally more water was lost through soil evaporation over the pulse period in the native grass community. Interestingly, this pattern contrast with observations from the previous year under similar experimental conditions (Huxman et al., 2004b).

Soil wetting by irrigation produced a rapid increase in ET that reached maximum rates on D3 (Fig. 3). ET rates over the 15-day period in stands of *H. contortus* were low compared to those in stands of *E. lehmanniana* ( $p = 0.028$ ; species by time interaction; MANOVA repeated measurements analysis). The contrasting ET rates among stands of both species were reflected in soil water storage. Low ET rates in stands of *H. contortus*

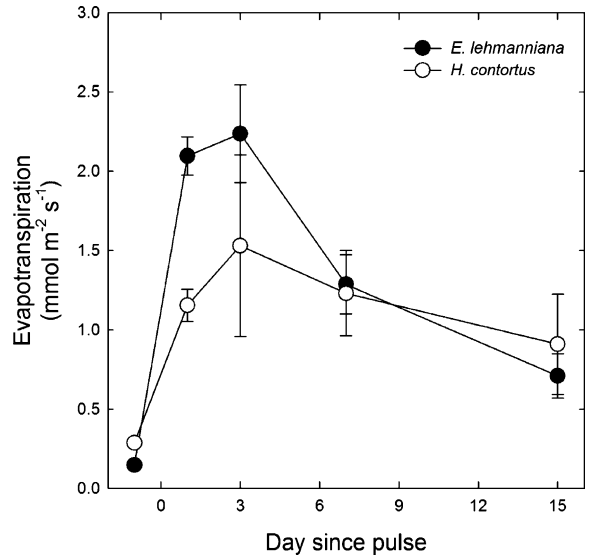


Fig. 3. Daytime evapotranspiration rates in experimental stands of *E. lehmanniana* and *H. contortus* following an experimental irrigation of 39 mm. Bars are standard errors of the mean ( $n = 3$ ).

maintained higher soil moisture content than in stands of *E. lehmanniana* (Fig. 2).

#### 3.2. Plant responses to the irrigation pulse

The moisture pulse produced a rapid ecophysiological response in *E. lehmanniana*. Shoot water potentials in this invasive grass rapidly shifted from very negative values on D-1 ( $< -5$  MPa) to an average of  $-0.9 \pm 0.5$  MPa on D1 and  $-1.4 \pm 0.6$  on D3. In contrast, the response of *H. contortus* was less pronounced. Shoot water potentials only rose to  $-1.7 \pm 0.5$  and  $-1.8 \pm 0.6$  on D1 and D3, respectively, in this native grass. Similarly, the isotopic composition of stem water revealed greater uptake of the labeled irrigation water in stands of *E. lehmanniana* compared to stands of *H. contortus*. Based on a simple, two-ended linear mixing relationship  $92 \pm 3.5\%$  of the *E. lehmanniana* transpiration water on D3 was from the irrigation pulse and only  $82 \pm 3.9\%$  of transpiration water was from the irrigation pulse in *H. contortus*. *H. contortus* apparently had limited physiological recovery from antecedent drought conditions.

The average plant density in vegetated stands was  $16 \pm 1.7$  and  $17 \pm 1$  plants per plot for *H. contortus* and *E. lehmanniana*, respectively. Despite the similarities in plant density, two important structural differences were evident between stands of the two species. In stands of *E. lehmanniana* green LAI was higher, in these stands the mean green LAI was  $0.66 \pm 0.20 \text{ m}^2 \text{m}^{-2}$  compared

to an average of  $0.37 \pm 0.05 \text{ m}^2 \text{ m}^{-2}$  in stands of *H. contortus*. Conversely, dead standing biomass and ground litter cover was much higher in stands of *H. contortus* (authors personal observation) than in stands of *E. lehmanniana*. Differences in canopy light interception among stands of both species and differences in soil temperature (at 5 cm depth) indirectly supported our observation. The mean canopy light interception in stands of *E. lehmanniana* was

Table 1

Geometric mean regression parameters for Keeling plots of water vapor produced in three stands of *E. lehmanniana* during morning (a.m.) and afternoon (p.m.) of several days following the water pulse

	Slope	y-intercept	$r^2$	$p$
Day 1				
Stand 1				
a.m.	$(-940.7 \pm 51.9)$	<b>+67.7</b> $\pm 3.2$	0.99	0.004
p.m.	$(-707.0 \pm 42.6)$	<b>+72.9</b> $\pm 3.3$	0.99	0.001
Stand 2				
a.m.	$(-756.7 \pm 80.0)$	<b>+87.9</b> $\pm 6.9$	0.97	0.003
p.m.	–	–	–	–
Stand 3				
a.m.	$(-1227.5 \pm 82.4)$	<b>+83.9</b> $\pm 5.3$	0.98	0.007
p.m.	$(-892.8 \pm 81.7)$	<b>+86.3</b> $\pm 5.5$	0.97	0.002
Day 3				
Stand 1				
a.m.	$(-1098.7 \pm 121.7)$	<b>+94.3</b> $\pm 8.1$	0.96	0.003
p.m.	$(-842.4 \pm 38.0)$	<b>+81.3</b> $\pm 2.0$	0.99	0.001
Stand 2				
a.m.	$(-1158.5 \pm 91.4)$	<b>+100.3</b> $\pm 7.2$	0.98	0.001
p.m.	$(-943.3 \pm 141.8)$	<b>+90.7</b> $\pm 11.8$	0.93	0.008
Stand 3				
a.m.	$(-1037.4 \pm 45.3)$	<b>+89.4</b> $\pm 3.2$	0.99	0.001
p.m.	$(-1059.4 \pm 137.1)$	<b>+85.7</b> $\pm 10.8$	0.95	0.005
Day 7				
Stand 1				
a.m.	$(-690.1 \pm 110.4)$	<b>+30.7</b> $\pm 9.2$	0.92	0.009
p.m.	$(-871.6 \pm 127.5)$	<b>+40.1</b> $\pm 12.2$	0.93	0.007
Stand 2				
a.m.	$(-649.6 \pm 87.7)$	<b>+36.2</b> $\pm 8.9$	0.94	0.006
p.m.	$(-757.6 \pm 107.0)$	<b>+22.6</b> $\pm 10.4$	0.94	0.006
Stand 3				
a.m.	$(-792.3 \pm 176.0)$	<b>+53.7</b> $\pm 15.9$	0.85	0.025
p.m.	$(-882.0 \pm 143.8)$	<b>+53.6</b> $\pm 13.5$	0.94	0.026
Day 15				
Stand 1				
a.m.	$(-431.0 \pm 105.9)$	<b>-44.2</b> $\pm 10.3$	0.81	0.040
Stand 2				
a.m.	$(-230.0 \pm 107.1)$	<b>-71.2</b> $\pm 13.1$	0.35	0.290
Stand 3				
a.m.	$(-306.9 \pm 132.3)$	<b>-56.6</b> $\pm 14.5$	0.44	0.220

The y-intercept in all regressions (bold;  $n = 5$ ) represents the isotopic composition ( $^2\text{H}$ ) of the *ET* flux ( $\delta_{\text{ET}}$ ).

$34 \pm 8\%$  versus  $50 \pm 18\%$  in stands of *H. contortus*. Soil temperatures at 5 cm depth in stands of *H. contortus* were on average  $5^\circ\text{C}$  cooler during gas exchange measurements than in soils from stands of *E. lehmanniana*. The limited physiological recovery, low green LAI and the cooling effect of the dead standing biomass and litter cover in plots of *H. contortus* may explain the lower *ET* rates in these stands (Fig. 3; Murphy et al., 2004).

Table 2

Geometric mean regression parameters for Keeling plots of water vapor produced in three stands of *H. contortus* during morning (a.m.) and afternoon (p.m.) periods on several days following a 39-mm irrigation pulse

	Slope	y-intercept	$r^2$	$p$
Day 1				
Stand 1				
a.m.	$(-633.2 \pm 132.9)$	<b>+27.6</b> $\pm 8.1$	0.87	0.021
p.m.	$(-280.5 \pm 35.6)$	<b>+17.5</b> $\pm 5.0$	0.95	0.004
Stand 2				
a.m.	$(-544.2 \pm 21.9)$	<b>+12.5</b> $\pm 2.0$	0.99	0.009
p.m.	$(-251.4 \pm 67.1)$	<b>+7.8</b> $\pm 8.4$	0.78	0.045
Stand 3				
a.m.	$(-981.5 \pm 125.2)$	<b>+47.1</b> $\pm 9.4$	0.95	0.005
p.m.	$(-384.9 \pm 32.6)$	<b>+37.0</b> $\pm 4.3$	0.98	0.001
Day 3				
Stand 1				
a.m.	$(-1021.0 \pm 92.0)$	<b>+81.3</b> $\pm 6.3$	0.98	0.002
p.m.	$(-735.1 \pm 60.3)$	<b>+64.1</b> $\pm 4.8$	0.98	0.001
Stand 2				
a.m.	$(-633.8 \pm 92.7)$	<b>+35.5</b> $\pm 8.9$	0.94	0.007
p.m.	$(-409.7 \pm 59.2)$	<b>+26.1</b> $\pm 6.2$	0.94	0.007
Stand 3				
a.m.	$(-530.0 \pm 44.0)$	<b>+24.2</b> $\pm 4.4$	0.98	0.001
p.m.	$(-599.4 \pm 86.5)$	<b>+37.7</b> $\pm 7.5$	0.94	0.007
Day 7				
Stand 1				
a.m.	$(-761.4 \pm 77.7)$	<b>+46.4</b> $\pm 7.0$	0.97	0.003
p.m.	$(-818.0 \pm 143.8)$	<b>+36.7</b> $\pm 12.9$	0.90	0.012
Stand 2				
a.m.	$(-559.2 \pm 93.3)$	<b>+21.5</b> $\pm 9.7$	0.91	0.011
p.m.	$(-486.0 \pm 34.2)$	<b>+5.5</b> $\pm 3.7$	0.98	0.001
Stand 3				
a.m.	$(-623.4 \pm 127.9)$	<b>+31.0</b> $\pm 11.9$	0.87	0.019
p.m.	$(-736.5 \pm 101.3)$	<b>+32.7</b> $\pm 8.3$	0.94	0.006
Day 15				
Stand 1				
a.m.	$(-265.3 \pm 132.4)$	<b>-64.2</b> $\pm 17.0$	0.25	0.387
Stand 2				
a.m.	$(-179.2 \pm 84.5)$	<b>-59.0</b> $\pm 7.8$	0.33	0.308

The y-intercept in all regressions (bold;  $n = 5$ ) represents the isotopic composition ( $^2\text{H}$ ) of the *ET* flux ( $\delta_{\text{ET}}$ ).

3.3. Isotopic composition of sources contributing to ET

The isotopic compositions of component fluxes contributing to ET were easily distinguishable over the pulse period.  $\delta_E$  was more depleted in heavy isotopes than  $\delta_T$  in all cases, but absolute differences were not constant between morning and afternoon periods, species or collection days (Tables 4 and 5).  $\delta_E$  was 5–10‰ more depleted in  $^2\text{H}$  on D1 and D3 in stands of *H. contortus* than in stands of *E. lehmanniana* as a result of cooler soil temperatures since the isotopic composition of soil water at the evaporation front was alike in all stands (Fig. 2). This trend was reversed on D7 as a result of less enriched  $\delta_L$  values in *E. lehmanniana* stands.

Despite contrasting patterns of physiological recovery from previous drought (Section 3.2), our modeling approach to calculate  $\Delta T$  (Eq. (4)) revealed similar daily trends in both grass species through the pulse period (Tables 4 and 5). In general, grasses did not transpire at

isotopic steady state (ISS;  $\delta_S = \delta_T$  or  $\Delta T = 0$ ) in the morning but rapidly approached and remained near ISS during the afternoon. The magnitude of deviation from ISS in the morning was not constant across different measurement days.  $\delta_T$  during morning periods was more depleted in heavy isotopes than  $\delta_S$  by 13–26‰ on D1, 4 to 10‰ on D3 and 5–8‰ on D7 (Tables 4 and 5). In all cases  $\delta_T$  was about 1‰ more enriched than  $\delta_S$  in the afternoon.

3.4. Partitioning of ET based on Keeling plots of water vapor

Significant ( $\alpha = 0.05$ ) linear relationships between increments of vapor concentration inside the chamber and the isotopic composition ( $\delta^2\text{H}$ ) of vapor collected at different time intervals during the gas exchange measurements were found for all Keeling plots produced in vegetated stands on D1, D3 and D7 (mean  $r^2 \pm \text{S.D.} = 0.94 \pm 0.05$ ,  $n = 35$ ; Tables 1 and 2), and in one case in stands of *E. lehmanniana* (stand 1) on D15

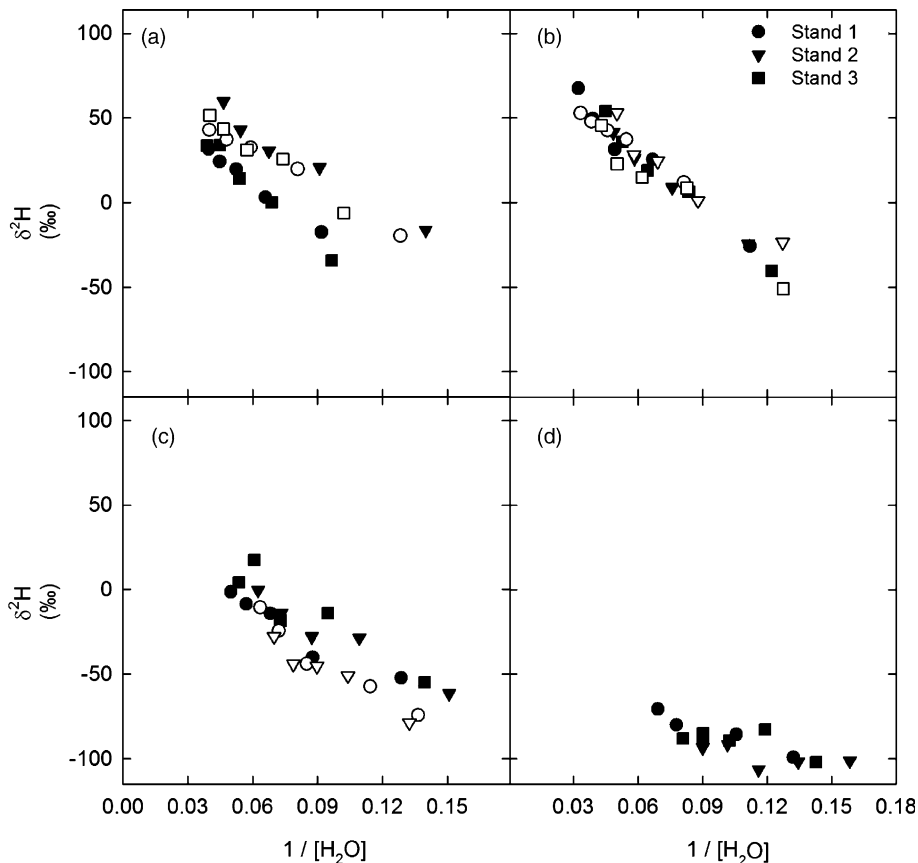


Fig. 4. Daytime Keeling plots of water vapor collected inside a large static chamber covering experimental stands of *Eragrostis lehmanniana* on days 1 (a), 3 (b), 7 (c) and 15 (d) following an irrigation of 39 mm. Different symbols represent different stands. Dark symbols correspond to vapor collected between 8:30 and 11:30 h and open symbols are for vapor collected between 14:00 and 16:30 h. Regression parameters are shown in Table 1.

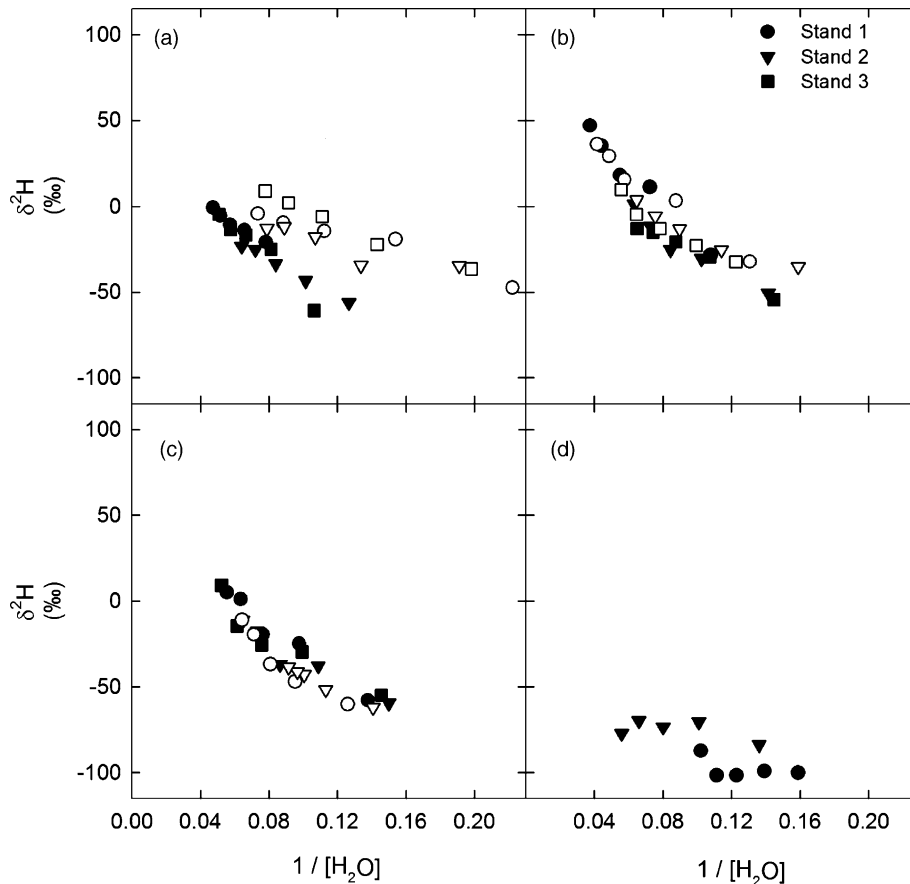


Fig. 5. Daytime Keeling plots of water vapor collected inside a large static chamber covering experimental stands of *Heteropogon contortus* on days 1 (a), 3 (b), 7 (c) and 15 (d) following an irrigation of 39 mm. Different symbols represent different stands. Dark symbols correspond to vapor collected between 8:30 and 11:30 h and open symbols are for vapor collected between

(Table 1). Slopes of most Keeling plots on D15 were not statistically different from zero for both species (Figs. 4d and 5d). The lack of linear fit in Keeling plot regressions and consistency of values for the y-intercepts of both species ( $\sim -60\text{‰}$ ; Tables 1 and 2) suggests that  $\delta_{ET}$  was similar to the isotopic composition of the atmospheric background vapor under the rain-out shelters. If this was true, then E dominated the ET flux since the average ( $n = 3$ ) isotopic composition of stem water in *E. lehmanniana* on D15 was still highly enriched in  $^2\text{H}$  ( $+61 \pm 20\text{‰}$ ).

Values of  $\delta_{ET}$  in stands of *E. lehmanniana* always fell between values of  $\delta_T$  and  $\delta_E$  on D1, D3 and D7 (Tables 1 and 4).  $T/ET$  in these stands was determined from Eq. (1), except on D15 when we were unable to determine  $\delta_E$ . The  $T/ET$  values for individual plots of *E. lehmanniana* were similar within each measurement day and no consistent differences were evident between morning and afternoon periods (Table 4). Mean daily values of  $T/ET$  varied from  $0.35 \pm 0.07$  on D1 to  $0.43 \pm 0.08$  on D3, but decreased to

Table 3

Geometric mean regression parameters for Keeling plots of water vapor produced in stands free of vegetation during the morning (a.m.) and afternoon (p.m.) of D3 and D7 after the irrigation pulse

	Slope	y-intercept	$r^2$	$p$	$\delta_E$
Day 3					
Stand 1					
a.m.	$(-738.7 \pm 81.2)$	<b>+66.9</b> $\pm 9.5$	0.96	0.003	63.5
p.m.	$(-747.4 \pm 147.2)$	<b>+61.9</b> $\pm 15.2$	0.88	0.018	68.9
Stand 2					
a.m.	$(-723.43 \pm 147.7)$	<b>+66.7</b> $\pm 15.6$	0.87	0.019	62.8
p.m.	$(-580.50 \pm 205.8)$	<b>+36.1</b> $\pm 26.0$	0.62	0.11	66.3
Day 7					
Stand 1					
a.m.	$(-798.0 \pm 212.2)$	<b>+51.2</b> $\pm 32.9$	0.78	0.044	55.6
p.m.	$(-1117.5 \pm 107.9)$	<b>+60.7</b> $\pm 16.3$	0.97	0.002	60.0
Stand 2					
a.m.	$(-451.3 \pm 159.7)$	<b>-13.9</b> $\pm 26.6$	0.62	0.111	45.7
p.m.	$(-1034.7 \pm 125.6)$	<b>+48.7</b> $\pm 19.0$	0.95	0.004	51.3

The y-intercept (bold) represents the isotopic composition ( $^2\text{H}$ ) of the entire flux. In all regressions,  $n = 5$ .  $\delta_E$  is the isotopic composition of soil evaporation (Eq. (5)).

Table 4  
Measured and modeled isotopic compositions ( $^2\text{H}$ ) of ecosystem water sources contributing to ET in three stands of *E. lehmanniana*

	$g$ ( $\text{mol m}^{-2} \text{s}^{-1}$ )	$\delta_S$ (‰)	$\Delta_{es}$ (‰)	$\Delta_{en}$ (‰)	$\Delta T$ (‰)	$\delta_T$ (‰)	$\delta_E$ (‰)	$T/ET$
Day 1								
Stand 1								
a.m.	0.038	115	93	68	-26	89	60.7	$0.25 \pm 0.06$
p.m.	0.071		79	80	1	116	60.5	$0.22 \pm 0.06$
Stand 2								
a.m.	0.020	127	86	63	-22	105	63.0	$0.60 \pm 0.10$
p.m.	0.050		78	80	1	128	52.5	–
Stand 3								
a.m.	0.053	124	87	73	-13	111	71.0	$0.31 \pm 0.09$
p.m.	0.041		78	80	2	126	66.9	$0.33 \pm 0.09$
Day 3								
Stand 1								
a.m.	0.085	134	85	76	-10	124	59.6	$0.54 \pm 0.10$
p.m.	0.087		78	79	1	134	67.2	$0.21 \pm 0.03$
Stand 2								
a.m.	0.046	121	80	70	-10	111	71.0	$0.74 \pm 0.12$
p.m.	0.135		78	79	0	121	68.9	$0.42 \pm 0.19$
Stand 3								
a.m.	0.135	125	79	75	-4	121	69.0	$0.39 \pm 0.05$
p.m.	0.103		78	79	1	125	70.3	$0.28 \pm 0.17$
Day 7								
Stand 1								
a.m.	0.069	111	82	74	-8	103	15.8	$0.17 \pm 0.09$
p.m.	0.039		82	84	2	113	20.0	$0.22 \pm 0.12$
Stand 2								
a.m.	0.124	100	81	77	-5	95	-5.4	$0.42 \pm 0.08$
p.m.	0.063		81	82	1	101	-8.2	$0.28 \pm 0.10$
Stand 3								
a.m.	0.106	105	81	76	-6	99	50.5	$0.07 \pm 0.16$
p.m.	0.082		81	82	1	106	44.7	$0.15 \pm 0.22$

$\delta_T$  is the isotopic composition of transpiration after accounting for potential deviations from isotopic steady state.  $\delta_S$  is the isotopic composition of water from basal culms and  $\delta_E$ , the isotopic composition of soil evaporation (Eq. (5)).  $g$  is stomatal conductance.  $\Delta_{en}$ ,  $\Delta_{es}$  and  $\Delta T$  are modeled outputs from Eqs. (2)–(4), respectively (see Section 2.3.2). Instantaneous  $T/ET$  during morning (a.m.) and afternoon (p.m.) periods were calculated from Eq. (1). The error on  $T/ET$  was determined from errors in the y-intercept from Keeling plots and the variability of the sources based on Phillips and Gregg (2001).

$0.22 \pm 0.05$  on D7. Assuming that *E. lehmanniana* transpire at ISS during the morning could underestimate  $T/ET$  by 8–21% on D1, by 3–15% on D3 and by about 2% on D7, while the impact during the afternoon would be on the order of only 1% for all days (Section 3.3; Table 4).

We were not able to calculate  $T/ET$  on D1 and D3 in stands of *H. contortus* because in most cases  $\delta_{ET}$  values did not fall between  $\delta_E$  and  $\delta_T$  (Eq. (1)). In these cases,  $\delta_{ET}$  was, on average, 25‰ more negative than  $\delta_E$ . However, on D7, the mean daily  $T/ET$  in *H. contortus* stands was  $0.09 \pm 0.03$  (Table 5). Notably, when we were able to resolve  $T/ET$  prior to D7 (stand 1, D3) the

ET rate was comparable to the rates in stands of *E. lehmanniana* (e.g. ET in this single case was  $2.2 \text{ mmol m}^{-2} \text{ s}^{-1}$ ; see error bars in Fig. 3). The difference in ET rates among stands of *H. contortus* on D3 ( $\sim 1 \text{ mmol m}^{-2} \text{ s}^{-1}$ ) was consistent with the magnitude of canopy transpiration in stand 1 during D3 ( $T/ET$  was 0.37 or  $0.82 \text{ mmol m}^{-2} \text{ s}^{-1}$  in this case; Table 5), suggesting that grass transpiration was responsible for the higher ET in this stand. Estimates of  $T/ET$  in stands of *H. contortus* were always lower during the afternoon, coinciding with a tendency towards lower values of stomatal conductance during the same periods (Table 5).

Table 5

Measured and modeled isotopic compositions ( $^2\text{H}$ ) of ecosystem water sources contributing to ET in three stands of *H. contortus* (see Table 4 for symbol codes)

	$g \text{ (mol m}^2 \text{ s}^{-1}\text{)}$	$\delta_S \text{ (‰)}$	$\Delta_{es} \text{ (‰)}$	$\Delta_{en} \text{ (‰)}$	$\Delta T \text{ (‰)}$	$\delta_T \text{ (‰)}$	$\delta_E \text{ (‰)}$	$T/ET$
Day 1								
Stand 1								
a.m.	0.050	104	85	71	-14.3	90	55.6	-
p.m.	0.049		79	80	0.9	105	48.9	-
Stand 2								
a.m.	0.022	100	85	63	-22.1	78	45.3	-
p.m.	0.100		79	79	0.4	100	42.9	-
Stand 3								
a.m.	0.014	98	85	59	-26.5	72	59.1	-
p.m.	0.043		78	79	0.8	99	49.7	-
Day 3								
Stand 1								
a.m.	0.080	114	84	74	-9.6	104	51.6	$0.57 \pm 0.09$
p.m.	0.101		78	79	0.4	114	53.1	$0.22 \pm 0.07$
Stand 2								
a.m.	0.056	112	81	71	-9.9	102	57.3	-
p.m.	0.108		78	79	0.4	112	60.2	-
Stand 3								
a.m.	0.048	100	78	70	-8.7	91	51.1	-
p.m.	0.075		78	79	0.5	100	51.8	-
Day 7								
Stand 1								
a.m.	0.118	100	82	76	-5.5	94	35.2	$0.16 \pm 0.10$
p.m.	0.102		82	82	0.4	100	36.0	$0.01 \pm 0.17$
Stand 2								
a.m.	0.135	110	81	77	-4.9	105	3.8	$0.18 \pm 0.08$
p.m.	0.103		80	81	0.5	111	5.0	$0.01 \pm 0.03$
Stand 3								
a.m.	0.149	103	81	77	-4.5	99	21.0	$0.12 \pm 0.13$
p.m.	0.126		81	82	0.4	103	28.3	$0.06 \pm 0.10$

Instantaneous  $T/ET$  during morning (a.m.) and afternoon (p.m.) periods were calculated from Eq. (1). The error on estimates of  $T/ET$  was determined from errors in the y-intercept from Keeling plots and the variability of the sources based on Phillips and Gregg (2001).

Soil evaporation was likely the dominant component of ET in stands of *H. contortus* where  $T/ET$  was unresolved since Keeling plots indicated a  $\delta_{ET}$  value that was far more depleted in heavy isotopes than  $\delta_T$  and the grass did not appear to fully recover from previous drought stress (Section 3.2). This observation is also consistent with changes in soil water content and the isotopic composition in the soil profile (Section 3.1; Fig. 2). Estimates of canopy transpiration in stands of *H. contortus* from scaled leaf-level measurements support this assertion. The mean ( $n = 3$ ) canopy transpiration rate from stands of *H. contortus* on D1 was only  $0.12 \pm 0.01 \text{ mmol m}^2 \text{ s}^{-1}$  (e.g. about 10% of the ET flux). This value is within the standard error of estimates of  $T/ET$  determined from isotopic measurements (Table 5).

### 3.5. Method validation

Mean soil evaporation rates in stands free of vegetation were  $0.8 \pm 0.1 \text{ mmol m}^2 \text{ s}^{-1}$  ( $\pm$ S.D.,  $n = 2$ ) on D3 and decreased to  $0.3 \pm 0.03 \text{ mmol m}^2 \text{ s}^{-1}$  on D7. Keeling plot regressions from these stands were linear except in two cases (Fig. 6).  $\delta_{ET}$  values from Keeling plots produced in these bare-soil plots were similar to modeled  $\delta_E$  values (Table 3). In six of the eight cases, measured values of  $\delta_{ET}$  based on the Keeling plots were only slightly different than the modeled values (Table 3).

Estimates of stand transpiration in *E. lehmanniana* based on ET rates and  $T/ET$  calculations from isotopic measurements were somewhat higher than estimates of stand transpiration from leaf-to-canopy scaling. This

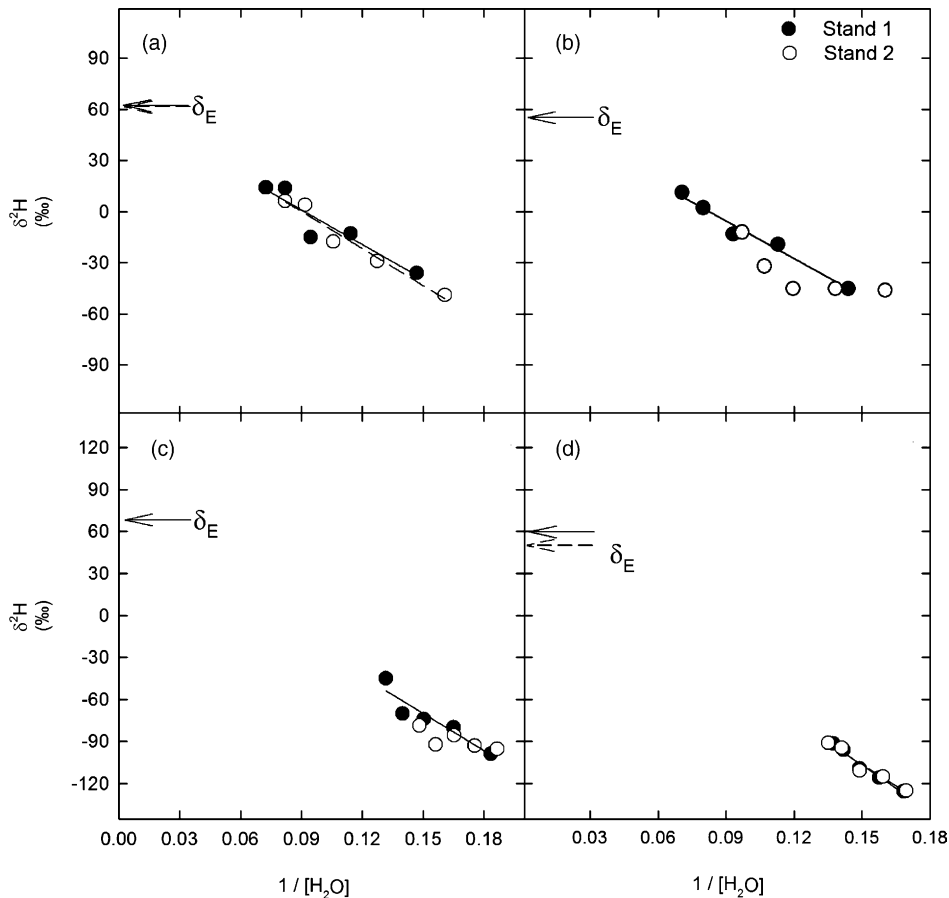


Fig. 6. Keeling plots of water vapor collected inside a large static chamber covering stands free of vegetation on days 3 ((a) a.m.; (c) p.m.) and 7 ((b) a.m.; (d) p.m.) following an irrigation of 39 mm. Different symbols represent different experimental stands. Arrows indicate the modeled isotopic value (Eq. (5)) of the soil evaporation flux ( $\delta_E$ ). Regression parameters are shown in Table 3.

was particularly the case on D1 (Fig. 7). However, both approaches appear to capture the dynamics of transpiration throughout the pulse period; estimates from both methods were positively correlated (Pearson's  $r = 0.76$ ,  $p = 0.0004$ ,  $n = 17$ ; Fig. 7) and ranks were maintained for each time combination (e.g. pulse day and morning versus afternoon). There were insufficient data to show this relationship for *H. contortus* but overall estimates tend to agree on the contrast between morning and afternoon transpiration rates (Fig. 7).

The isotopic composition of water from grass stems was generally lower than  $\delta^2\text{H}$  of soil water at the evaporation front (Fig. 8). This correlation was positive for stands of *E. lehmanniana* (Pearson's  $r = 0.75$ ,  $p = 0.018$ ,  $n = 9$ ), but no statistically significant correlation was found for *H. contortus* (Pearson's  $r = 0.03$ ,  $p = 0.9$ ,  $n = 9$ ). The differences between  $\delta^2\text{H}$  of stem water and soil water at the evaporation front was possibly because grass roots extended below the soil

layers that we sample as the evaporation front (or even below 30 cm) and the grass was using some water more depleted in the heavy isotope.

#### 4. Discussion

The use of Keeling plots of water vapor to partition ET until now has been restricted to large-scale ecosystem studies using sampling within the open boundary layer (Moreira et al., 1997; Wang and Yakir, 2000; Helliker et al., 2002; Yopez et al., 2003; Williams et al., 2004). Here, we have illustrated the application of the Keeling plot method using large gas exchange chambers in experimental grassland plots. To our knowledge, this is the first time that Keeling plots of water vapor from plot-scale chambers have been reported. This is in remarkable contrast with  $\text{CO}_2$  studies for which Keeling plot chamber methods are commonly used to partition components of ecosystem

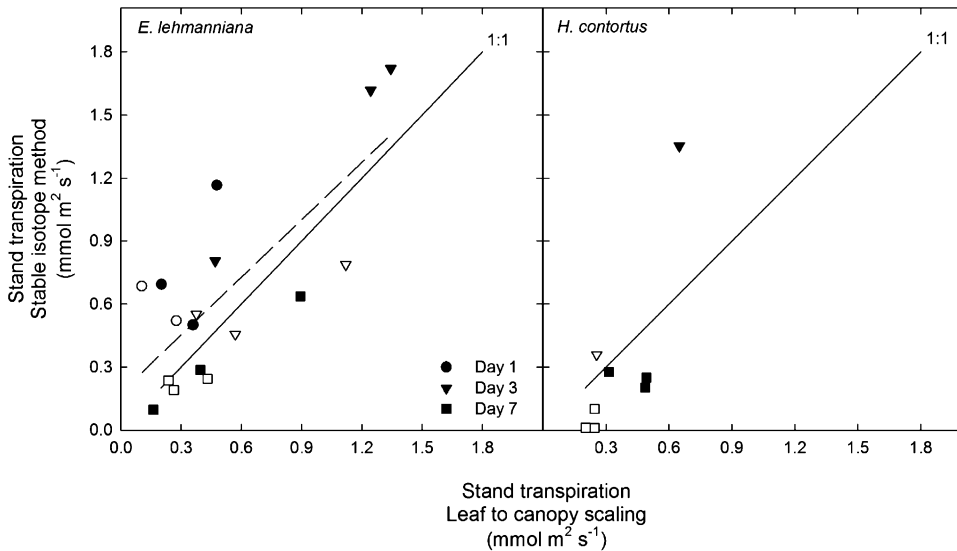


Fig. 7. Relationship between instantaneous rates of canopy transpiration calculated based on the stable isotope chamber method (y-axis) and canopy transpiration calculated from the leaf-to-canopy scaling (x-axis) along several days (different symbols) in stands of *E. lehmanniana* (left;  $n = 17$ ) and *H. contortus* (right;  $n = 8$ ). Dark symbols correspond to the morning and open symbols to the afternoon collection periods.

respiration (Flanagan and Ehleringer, 1998; Cable and Huxman, 2004). The chamber-based Keeling plot method proved to be useful for assessing the short-term dynamic response of  $T/ET$  in experimental grass stands under field conditions. High ET rates after irrigation produced large transient changes in water vapor concentration and isotope composition during the 6-min gas exchange measurements.

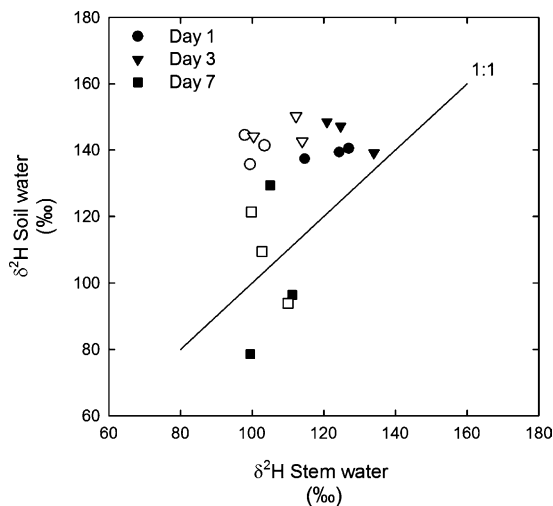


Fig. 8. Relationship between the isotopic composition of soil water at the evaporation front and the isotopic composition of water from basal grass culms over three dates following the experimental irrigation (e.g. different symbols). Dark symbols are for *E. lehmanniana* and open symbols are for *H. contortus*.

The inherent advantage of the Keeling plot method outlined here compared to other approaches is that it provides estimates of  $T/ET$  that are temporally and spatially compatible with parallel measurements of net ecosystem  $CO_2$  exchange using plot-sized chambers (e.g. Angell et al., 2001; Arnone and Obrist, 2003; Obrist et al., 2003; Huxman et al., 2004b). The combined measurements are potentially very useful for characterizing the biotic and abiotic factors underlying ecosystem-level water-use efficiency under rapidly changing conditions typical of arid and semiarid environments experiencing wet/dry transitions. Further, the chamber method is suitable for plot-scale experimental manipulations (e.g. litter removals, grazing exclosures, resource manipulations, etc.) and can be used with replicated experimental units, which allow statistical analysis. However, sufficient isotopic gradients necessary for Keeling plot analysis are difficult to obtain when soil conditions are dry and ET rates are low.

The use of irrigation water highly enriched with  $^2H$  resulted in a very distinct isotopic composition of ET. Although labeling is not required for this approach to work (Wang and Yakir, 2000) the use of labeled water provides a large contrast between the isotopic composition of ET and the background atmosphere. Preliminary measurements of stand gas exchange are recommended to verify that isotope and vapor concentration gradients can be generated for Keeling plots.

Leaf-to-canopy scaling in combination with chamber measurements of ET have been employed pre-

viously at our research site to calculate  $T/ET$  (Huxman et al., 2004b). Although this approach is suitable for this goal, estimates are prone to error. In the present study, estimates of stand transpiration based on the ET partitioning by Keeling plots in stands of *E. lehmanniana* were somewhat higher than the estimates from leaf-to-canopy scaling. Underestimations of LAI in the leaf-to-canopy scaling, poor spatial representation of  $g$  measurements (e.g. single leaf measurements), poor estimations of  $\delta_T$  under non-ISS conditions and/or temporal differences between measurements of  $g$  and stand-level gas exchange could account for these differences. Nevertheless, independent estimates of stand transpiration from both methods correlated well in stands of *E. lehmanniana*, providing support for the validity of the Keeling plot method.

#### 4.1. Method assumptions

Previous field and laboratory experiments concerned with factors controlling the isotopic composition of leaf water suggest that, during typical diurnal regimes of atmospheric humidity, leaf water is not always at ISS and that transpiration at ISS occurs only after ambient conditions are relatively stable (Flanagan et al., 1991; Wang and Yakir, 1995; Harwood et al., 1998; Lai et al., 2005; Farquhar and Cernusak, 2005; Pendall et al., 2005). These observations are of particular relevance in studies where the isotopic composition of transpiration vapor is a key parameter for isotopic mass balance partitioning of ET because the error for not accounting for deviations from ISS can be large (Lai et al., 2005). *E. lehmanniana* and *H. contortus* did not transpire at ISS during the morning, but transpiration at ISS was attained by midday and persisted through the afternoon. Failure to account for deviations of transpiration at ISS in our study would translate into an error of up to 20% in our final estimates of  $T/ET$ . The modeling scheme that we chose to calculate  $\delta_T$  could be further improved by considering isotopic heterogeneity of leaf water (Helliker and Ehleringer, 2000; Farquhar and Cernusak, 2005). For example, by accounting for differences in the isotopic composition of bulk leaf water and that at the sites of evaporation (e.g. accounting for a pécelet effect; Barbour and Farquhar, 2003).

Approaches for estimating  $\delta_E$  also could lead to error. Potential errors associated with our selection criteria of soil layers where liquid water was available for evaporation and modeling of fractionation appeared to be minor. The  $y$ -intercept of Keeling plots closely matched our modeled value of  $\delta_E$  in stands free of vegetation where  $\delta_E = \delta_{ET}$ . An alternative approach for

identifying the evaporation front in the calculation of  $\delta_E$  is to assume that the isotopic composition of plant source water represents that of water from soil layers where water is available for evaporation. This approach was used by Wang and Yakir (2000) under very humid conditions where little change in the isotopic composition of soil water was assumed between rewetting events. However, this approach is prone to error under rapid drying conditions typical of semiarid regions and when the vegetation takes up water from several layers in the soil profile that may include water from below the evaporation front. The use of stem water values as a proxy for  $\delta_L$  in the calculations of  $\delta_E$  substantially affect estimates of  $T/ET$  in our experimental grassland system.

Further investigations are needed to select valid parameters for an accurate expression of  $\delta_E$  under different circumstances. For example, our inability to calculate  $T/ET$  in stands of *H. contortus* during periods of low transpiration early in the pulse period may be partially related to unaccounted effects of a wet thick litter layer on the estimation of  $\delta_E$  (e.g. interception, poor mixing, nighttime condensation). Litter intercepts and absorbs significant amounts of water (Sato et al., 2004) and controls evaporation rates (Murphy et al., 2004). In our experiment, the litter layer may have acted as the source of evaporation contributing an isotopic signal distinct from the one expected from the isotopic composition of soil water. Differences in temperature of soil and litter and its influence on the equilibrium fractionation (Majoube, 1971), the varying contributions of turbulent and diffusive transport through these media and nighttime condensation in the litter layer should be considered to improve estimates of  $\delta_E$  when a wet litter layer is present.

Three additional assumptions underlie the application of the chamber Keeling plot method for ET partitioning: (1) only two sources contribute to ET; (2) the relative contribution of the two sources does not change during the analysis period; and (3) there is no loss of water vapor other than by turbulent mixing with the air (e.g. no condensation occurs) (Yakir and Sternberg, 2000). The first assumption is met with the chamber method since the experimental unit delimited by the chamber during gas exchange measurements contained only bare soil and grasses. In relation to other techniques where the Keeling plot partitioning is employed (Yopez et al., 2003), this represents an advantage because it avoids the problem of flux contamination from adjacent areas (Williams et al., 2004). Condensation likely did not occur during chamber sampling. Despite high ET rates on days immediately following the irrigations, dew-point

temperatures inside the gas exchange system during measurements never approached ambient air temperatures.

The chamber-based method outlined in Arnone and Obrist (2003) is very flexible for ET measurements at the plot scale (Obrist et al., 2003; Huxman et al., 2004b; see also Murphy et al., 2004). In such studies, daytime ET measurements are conducted during short time intervals (90–160 s) to avoid significant modification of the microenvironment. In our case, ET rates were measured over 6 min in order to allow enough time for collecting five vapor samples to produce Keeling plots. Relative humidity inside the chamber in most cases increased by 15% during this period. This change apparently did not substantially alter transpiration by the grasses or steady-state soil evaporation rates since the time traces of water vapor concentration were linear in all cases (data not shown). Keeling plots from D1 to D7 also were linear, suggesting that the relative contribution of transpiration and evaporation did not change over the 6-min measurement period. Furthermore, by using an isotopic non-steady state model of transpiration (Farquhar and Cernusak, 2005), an effect of 15% change in  $h$  during the instantaneous chamber measurement periods should not substantially affect  $\delta_T$  since these values are largely dependent on the isotopic composition of leaf water which, depending on its turnover time in the leaf, is controlled by antecedent environmental conditions (Cernusak et al., 2002; Lai et al., 2005; Pendall et al., 2005).

Other considerations regarding the method include the efficiency of the vapor trapping system. In order to collect vapor circulating in the traps at a flow rate of  $3 \text{ L min}^{-1}$  without compromising trapping efficiency, we made two modifications to the glass traps originally outlined by Helliker et al. (2002). We increased the trap length to 25 cm and filled the 6 mm inner tube with an 18 cm long column made with 3 mm glass beads. Such modifications allowed us to collect all the vapor circulating through the traps for the isotope analysis without significant flow restrictions in the gas exchange system. Attention to these issues is required if the chamber method is used in more humid conditions where, perhaps, enough water for the isotope analysis can be collected in a shorter amount of time or at lower flow rates.

## 5. Conclusion

Empirical estimates of  $T/ET$  advances the mechanistic understanding of how vegetation influences ecosystem processes like carbon and water exchange.

Characterizing the rapid changes in plant transpiration and soil evaporation during dynamic wetting and drying cycles following precipitation events is useful for identifying the biotic and abiotic factors controlling variation in ecosystem production in semiarid environments. Estimates of  $T/ET$  can be obtained using Keeling plots of water vapor produced under transient conditions inside large static chambers in the field. This is the first time that Keeling plots of water vapor are produced with the aid of a chamber for ecosystem studies. In general, the method proved to be quite robust for estimating  $T/ET$  under different soil moisture and plant physiological conditions during the first week following an experimental irrigation. However, the method is limited under very dry conditions when isotope and/or vapor concentration gradients are absent during the measurement periods. Also, our results suggest that further investigation is needed to appropriately define the parameters required in the calculation of the isotopic composition of the soil evaporation flux when a dense wet litter layer is present. Nevertheless, the method described here is suitable for plot or patch-scale experimental manipulations, which in combination with simultaneous measurements of  $\text{CO}_2$  and water exchange provide a unique tool to characterize the biotic and abiotic factors underlying ecosystem-level water-use efficiency at matched scales.

## Acknowledgments

This work was supported by the USDA-CSREES (Grant #00-35101-9308), the SAHRA-NSF Science and Technology Center (Agreement No. EAR-9876800) and NSF awards DEB-041-5977 and 041-8134 to TEH, DGW and JFW. We thank Michael Mason for help with the irrigation and soil water collection, Mark Larson for help with isotope analysis and Jessica Cable and Daniel Potts for their effort during the field campaigns. EAY was supported by CONACYT-Mexico under the graduate fellowship no. 150496.

## References

- Angell, R.R., Svejcar, T., Bates, J., Saliendra, N.Z., Johnson, D.A., 2001. Bowen ratio and closed chamber carbon dioxide flux measurements over sagebrush steppe vegetation. *Agric. For. Met.* 108, 153–161.
- Arnone III, J.A., Obrist, D., 2003. A large daylight geodesic dome for quantification of whole-ecosystem  $\text{CO}_2$  and water vapor fluxes in arid shrublands. *J. Arid Environ.* 55, 629–643.
- Austin, A.T., Yahdjian, L., Stark, J.M., Belnap, J., Porporato, A., Norton, U., Ravetta, D., Schaeffer, S., 2004. Water pulses and

- biogeochemical cycles in arid and semiarid ecosystems. *Oecologia* 141, 221–235.
- Barbour, M.M., Farquhar, G.D., 2003. Do pathways of water movement and leaf anatomical dimensions allow development of gradients in  $H_2^{18}O$  between veins and the sites of evaporation within leaves? *Plant Cell Environ.* 24, 107–121.
- Cable, J.M., Huxman, T.E., 2004. Precipitation pulse size effects on Sonoran Desert soil microbial crusts. *Oecologia* 141, 317–324.
- Cappa, C.D., Hendricks, M.B., DePalo, D.J., Cohen, R.C., 2003. Isotopic fractionation of water during evaporation. *J. Geophys. Res.* 108, 4525, doi:10.1029/2003JD003597.
- Cernusak, L.A., Pate, J.S., Farquhar, G.D., 2002. Diurnal variation in the stable isotope composition of water and dry matter in fruiting *Lupinus angustifolius* under field conditions. *Plant, Cell Environ.* 25, 893–907.
- Coleman, M.L., Shepard, T.J., Durham, J.J., Rouse, J.E., Moore, G.R., 1982. Reduction of water with zinc for hydrogen isotope analysis. *Anal. Chem.* 54, 993–995.
- Craig, H., Gordon, L.I., 1965. Deuterium and oxygen-18 variations in the ocean and the marine atmosphere. In: Tongiorgi, E. (Ed.), *Proceedings of the Conference on Stable Isotopes in Oceanographic Studies, Paleotemperatures*. Laboratory of Geology and Nuclear Science, Pisa, pp. 9–130.
- Ehleringer, J.R., Roden, J., Dawson, T.E., 2000. Assessing ecosystem-level water relations through stable isotope ratio analysis. In: Sala, O.E., Jackson, R.B., Mooney, H.A., Howarth, R.W. (Eds.), *Methods in Ecosystem Science*. Springer, New York, pp. 181–198.
- English, N.B., Weltzin, J.F., Fravolini, A., Thomas, L., Williams, D.G., 2005. Design and performance of large-scale precipitation shelters in semi-desert grassland. Santa Rita Experimental Range, Arizona. *J. Arid Environ.* 63, 324–343.
- Farquhar, G.D., Cernusak, L.A., 2005. On the isotopic composition of the leaf water in the non-steady state. *Funct. Plant Biol.* 32, 293–303.
- Flanagan, L.B., Ehleringer, J.R., 1998. Ecosystem–atmosphere  $CO_2$  exchange: interpreting signals of change using stable isotope ratios. *Trends Ecol. Evol.* 13, 10–14.
- Flanagan, L.B., Comstock, J.P., Ehleringer, J.R., 1991. Composition of modeled and observed environmental influences on the stable oxygen and hydrogen isotope composition of leaf water in *Phaseolus vulgaris* L. *Plant Physiol.* 96, 588–596.
- Fravolini, A., Hultine, K.R., Brugnoli, E., Gazal, R., English, N.B., Williams, D.G., 2005. Precipitation pulse use by an invasive woody legume: the role of soil texture and pulse size. *Oecologia* 144, 618–627.
- Gat, J.R., 1996. Oxygen and hydrogen isotopes in the hydrological cycle. *Annu. Rev. Earth Planet Sci.* 24, 255–262.
- Harwood, K.G., Gillon, J.S., Griffiths, H., Broadmeadow, S.J., 1998. Diurnal variations of  $\Delta^{13}CO_2$ ,  $\Delta^{18}O^{16}O$  and evaporative site enrichment of  $\delta H_2^{18}O$  in *Pipper aduncum* under field conditions. *Plant Cell Environ.* 21, 269–283.
- Harwood, K.G., Gillon, J.S., Roberts, A., Griffiths, H., 1999. Determinants of isotopic coupling of  $CO_2$  and water vapour within a *Quercus petraea* forest canopy. *Oecologia* 119, 109–119.
- Helliker, B.R., Ehleringer, J.R., 2000. Establishing a grassland signature in veins:  $^{18}O$  in the leaf water of C3 and C4 grasses. *Proc. Nat. Acad. Sci.* 97, 7834–7898.
- Helliker, B.R., Roden, J.S., Cook, C., Ehleringer, J.R., 2002. A rapid and precise method for sampling and determining the oxygen isotope ratio of atmospheric water vapor. *Rapid Commun. Mass Spectrom.* 16, 929–932.
- Huxman, T.E., Snyder, K.A., Tissue, D., Leffler, A.J., Ogle, K., Pockman, W.T., Sandquist, D.R., Potts, D., Schwinning, S., 2004a. Precipitation pulses and carbon fluxes in semiarid and arid ecosystems. *Oecologia* 141, 254–268.
- Huxman, T.E., Cable, J.M., Ignace, D.D., Eilts, J.A., English, N.B., Weltzin, J.F., Williams, D.G., 2004b. Response of net ecosystem gas exchange to a simulated precipitation pulse in a semiarid grassland: the role of native versus non-native grasses and soil texture. *Oecologia* 141, 295–305.
- Huxman, T.E., Wilcox, B.P., Breshears, D.D., Scott, R.L., Snyder, K.A., Small, E.E., Hultine, K., Pockman, W.T., Jackson, R.B., 2005. Ecohydrological implications of woody plant encroachment. *Ecology* 86, 308–319.
- Keeling, C.D., 1961. The concentration and isotopic abundances of carbon dioxide and marine air. *Geochim. Cosmochim. Acta* 24, 277–298.
- Konukcu, F., Istanbuloglu, A., Kocaman, I., 2004. Determination of water content in drying soils: incorporating transition from liquid phase to vapour phase. *Aust. J. Soil Res.* 42, 1–8.
- Kostner, B., 2001. Evaporation and transpiration from forest in Central Europe—relevance of patch-level studies for spatial scaling. *Meteorol. Atmos. Phys.* 76, 69–82.
- Lai, C.T., Ehleringer, J.R., Bond, B.J., Paw U, K.T., 2005. Contributions of evaporation, isotopic non-steady state transpiration, and atmospheric mixing on the  $\delta^{18}O$  of water vapor in Pacific Northwest coniferous forest. *Plant Cell and Environ.*, doi:10.1111/j.1365-3040.2005.01402.x.
- Loik, M.E., Breshears, D.D., Lauenroth, W.K., Belnap, J., 2004. A multi-scale perspective of water pulses in dryland ecosystems: climatology and ecohydrology of the western USA. *Oecologia* 141, 181–269.
- Majoube, M., 1971. Fractionnement en oxygene-18 et en deuterium entre l'eau et sa vapaeur. *J. Chimie de Physique* 68, 1423–1436.
- Moncrieff, J.B., Jarvis, P.G., Valentini, R., 2000. Canopy fluxes. In: Sala, O.E., Jackson, R.B., Mooney, H.A., Howarth, R.W. (Eds.), *Methods in Ecosystem Science*. Springer, New York, pp. 161–180.
- Moreira, M.Z., Sternberg, L.S.L., Martinelli, L.A., Vctoria, R.L., Barbosa, E.M., Bonates, L.C.M., Nepstad, D.C., 1997. Contribution of transpiration to forest ambient vapour based on isotopic measurements. *Global Change Biol.* 3, 439–450.
- Murphy, S.R., Lodge, G.M., Harden, S., 2004. Surface soil water dynamics in pastures in northern New South Wales. 3. Evapotranspiration. *Aust. J. Exp. Agric.* 44, 571–583.
- Obrist, D., Delucia, E.H., Arnone III, J.A., 2003. Consequences of wildfire on ecosystem  $CO_2$  and water vapor fluxes in the Great Basin. *Global Change Biol.* 9, 563–574.
- Pearcy, R.W., Schulze, E.D., Zimmerman, R., 1989. Measurement of transpiration and leaf conductance. In: Pearcy, R.W., Ehleringer, J., Mooney, H.A., Rundel, P.W. (Eds.), *Plant Physiological Ecology*. Chapman & Hall, New York, pp. 137–160.
- Pendall, E., Williams, D.G., Leavitt, S., 2005. Comparison of measured and modeled variations in piñon pine leaf water isotopic enrichment across a summer moisture gradient. *Oecologia*, doi:10.1007/s00442-005-0164-7.
- Phillips, D.L., Gregg, J.W., 2001. Uncertainty in source partitioning using stable isotopes. *Oecologia* 127, 171–179.
- Reynolds, J.F., Kemp, P.R., Tenhunen, J.D., 2000. Effects of long-term variability on evapotranspiration and soil water distribution in the Chihuahuan Desert: a modeling analysis. *Plant Ecol.* 150, 45–159.
- Riley, W.J., Still, C.J., Helliker, B.R., Ribas-Carbo, M., Berry, J.A., 2003.  $^{18}O$  composition of  $CO_2$  and  $H_2O$  ecosystem pools and

- fluxes in a tallgrass prairie: simulations and comparisons to measurements. *Global Change Biol.* 9, 1567–1581.
- Sato, Y., Kumagai, T., Kume, A., Otsuki, K., Ogawa, S., 2004. Experimental analysis of moisture dynamics of litter layers—the effects of rainfall conditions and leaf shapes. *Hydrol. Process.* 18, 3007–3018.
- Scanlon, B.R., Levitt, D.G., Reedy, R.C., Keese, K.E., Sully, M.J., 2005. Ecological controls on water cycle response to climate variability. *Proc. Nat. Acad. Sci.* 102, 6033–6038.
- Sokal, R.R., Rohlf, F.J., 1995. *Biometry: the principles and practice of statistics in biological research.* W.H. Freeman and Company, New York.
- van de Griend, A.A., Owe, M., 1994. Bare soil surface resistance to evaporation by vapor diffusion under semiarid conditions. *Water Resour. Res.* 30, 181–188.
- Wang, X.F., Yakir, D., 1995. Temporal and spatial variations in the oxygen-18 content of leaf water in different plant species. *Plant Cell Environ.* 18, 377–1385.
- Wang, X.F., Yakir, D., 2000. Using stable isotopes of water in evaporation studies. *Hydrol. Process.* 14, 1407–1421.
- Wilson, K.B., Hanson, P.J., Mulholland, P.J., Baldocchi, D.D., Wullschlegel, S.D., 2001. A comparison of methods for determining forest evapotranspiration and its components: sap-flow, soil water budget, eddy covariance and catchment water balance. *Agric. For. Met.* 106, 153–168.
- Williams, D.G., Cable, W., Hultine, K., Hoedjes, J.C.B., Yopez, E.A., Simonneaux, V., Er-Raki, S., Boulet, G., de Bruin, H.A.R., Chehbouni, A., Hartogensis, O.K., Timouk, F., 2004. Components of evapotranspiration in an olive orchard determined by eddy covariance, sap flow and stable isotope techniques. *Agric. For. Met.* 125, 241–258.
- Whythers, K.R., Lauenroth, W.K., Paruelo, J.M., 1999. Bare soil evaporation under semiarid field conditions. *Soil Sci. Soc. Am. J.* 63, 1341–1349.
- Yakir, D., Sternberg, L.S.D., 2000. The use of stable isotopes to study ecosystem gas exchange. *Oecologia* 123, 297–311.
- Yamanaka, T., Yonetani, T., 1999. Dynamics of the evaporation zone in dry sandy soils. *J. Hydrol.* 217, 135–148.
- Yopez, E.A., Williams, D.G., Scott, R.L., Lin, G., 2003. Partitioning overstory and understory evapotranspiration in a semi-arid woodland ecosystem from the isotopic composition of water vapor. *Agric. For. Met.* 119, 53–68.